https://doi.org/10.32762/eygec.2025.26

FIBRE BRAGG GRATING STRAIN DATA FROM A CONCRETE JACKING PIPE

Asad WADOOD¹, Bryan A. McCABE², Brian B. SHEIL³

ABSTRACT

Microtunnelling or pipe jacking (PJ) is the preferred method of utility pipeline construction in congested urban environments due to its minimally disruptive nature. In this study, a 1490 mm outer diameter reinforced concrete (RC) jacking pipe was instrumented for incorporation within a 297 m long curved PJ drive as part of the Athlone Main Drainage Scheme in Ireland. Fibre Bragg grating (FBG) strain sensors were embedded at the four cardinal points of the pipe to measure axial and hoop strains. Additionally, two vibrating wire strain gauge pairs were installed at two cardinal points. In this paper, data collected from both sensor types during jacking are compared, and a preliminary analysis of the axial FBG strain data is provided.

Keywords: pipe jacking, microtunnelling, field monitoring, instrumentation, fibre Bragg grating strain sensors.

INTRODUCTION

The pipe jacking (PJ) technique is increasingly used in urban environments where underground pipelines need to be installed over great distances at relatively shallow depths, negotiating complex infrastructure and with restricted surface access. Wadood et al. (2025) reviewed eight PJ studies in which instrumented pipes were used to monitor the mechanical response of pipelines, most of which involved traditional vibrating wire strain gauges (VWSG). VWSGs can be difficult to manage as separate gauges are required at each sensing location. In contrast, fibre optic (FO) sensors facilitate multiple sensing locations along a cable length. FO sensors offer additional benefits over traditional strain sensors, such as immunity to water ingress and electromagnetic interference.

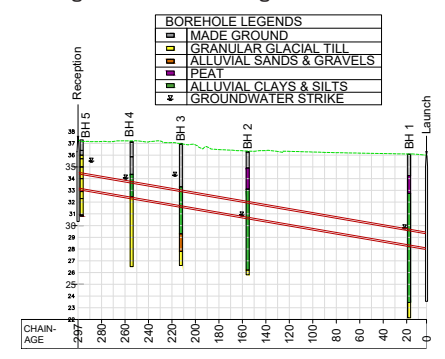


Figure 1 Vertical alignment of the drive

In this research, a reinforced concrete (RC) jacking pipe (1490 mm ext. dia.) was instrumented with fibre Bragg gratings (FBG) for deployment within a curved PJ drive in Athlone, Ireland. Four VWSGs were also installed. Axial strains from both gauge types are compared in this paper and some initial insight into the pipe's performance is provided.

PROJECT OVERVIEW

Athlone Main Drainage Scheme

The Athlone Main Drainage Scheme (ATHMDS) upgrade, which commenced in 2023, involves the construction of a 2.8 km long sewer network and two new stormwater overflows. These upgrades aim to eliminate sewer overflows into the River Shannon and increase the capacity of the network to support future population growth. Ward and Burke Construction Ltd. is the lead contractor on ATHMDS.

Drive details and ground conditions

The drive incorporating the instrumented pipe (IP1) was 297 m long, traversing the town centre of Athlone under existing roadways and close to buildings. The depth to pipe crown varied from 6.41 m at the start of the drive to 2.55 m at the end at a constant upward gradient of 1:58 (Fig. 1). The drive incorporated a horizontal curve with a radius of 500 m between chainages of 90.7 m and 264.3 m (Fig. 2).

¹ Civil Engineering, School of Engineering, University of Galway, Ireland, a.wadoodi@universityofgalway.ie

² Civil Engineering, School of Engineering, University of Galway, Ireland, bryan.mccabe@universityofgalway.ie

³ Laing O'Rourke Centre for Construction Engineering and Technology, University of Cambridge, United Kingdom. bbs24@cam.ac.uk



Figure 2 Horizontal alignment of the tunnel

The locations of the five boreholes (BH 1-5) relative to the pipeline are shown in Fig. 2, with the interpreted stratigraphy shown in Fig. 1. Generally, the ground conditions comprise made ground (0 - 2.9 m thick), underlain by peat (1.8 - 3.2 m), alluvial clays and silts (3 - 9 m) and granular glacial till (1 - 13 m). The tunnel passes through the alluvial clays and silts for the most part, with the granular glacial till encountered towards the end.

The tunnel boring machine (TBM) used was a Herrenknecht AVN 1200 (slurry shield machine) with an outer diameter of 1541 mm. Each RC pipe segment was 3 m long with outer and inner diameters of 1490 mm and 1200 mm respectively. The overcut thickness was 25.5 mm. IP1 was installed as pipe #31, 99 m behind the TBM outter face.

INSTRUMENTED PIPE PRODUCTION

Instrumentation scheme

The pipe was instrumented with four embedded FBG strain sensors at the cross section's cardinal points (N,S,E,W) in both the axial and hoop orientations (Fig. 3). Robustness of the fibre optic cables was ensured by specifying a 1 mm layer of glass fibre reinforced polymer (GFRP) and a 0.5 mm layer of high-density polyethylene (HDPE) coating. These were supplied by FBGS Technologies GmbH.

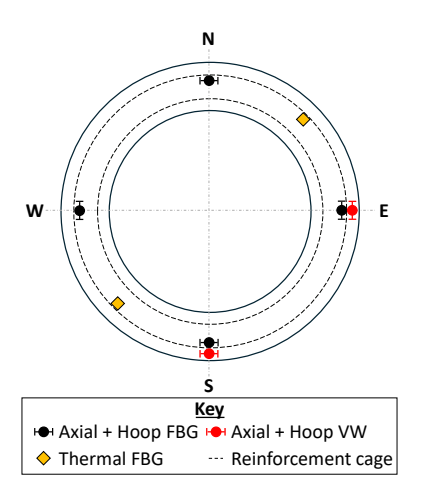


Figure 3 Schematic of sensor locations

Additionally, two pairs of embedded VWSGs with thermistors, supplied by Soil Instruments Ltd. (one axial, one hoop) were installed at the S and E cardinal points of the pipe to enable comparison with the FBG strains (Fig. 3).

Two FBGs were reserved for temperature measurements, hereafter referred to as 'thermal FBGs' (Fig. 3). To isolate them from mechanical effects, the method proposed by Hensman and Sheil (2023) was adopted, whereby each FBG was encapsulated in an aluminium block and subsequently wrapped in bubble wrap to isolate it from the concrete.

Fabrication

All jacking pipes utilised in the ATHMDS project were supplied by Tracey Concrete Ltd., Enniskillen, and were made of self-consolidating concrete with a 28-day cylinder strength of $\approx\!63$ MPa. The fabrication of IP1 can be summarised in the following steps.

- a. Fabrication of the inner and outer reinforcement cages (Fig. 3).
- b. Installation of sensors on the outer reinforcement cage (Fig. 4).
- c. Placement of inner and outer moulds.
- d. Casting of concrete.

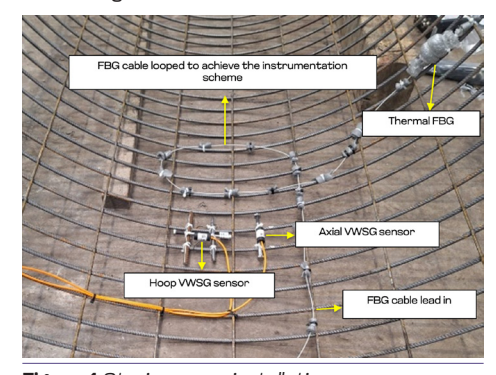


Figure 4 Strain sensor installation

Data Acquisition

The data acquisition system comprised a miniature computer and an uninterrupted power supply unit, housed within a watertight steel cabinet within IP1.

Separate loggers were used for FBG and VWSG sensors. The computer was connected to an Ethernet cable to allow real-time access to the data from outside the tunnel.

Data processing

FBGs are prefabricated gratings etched onto fibre optic cables and act as optical reflectors. When a light wave transmitted by the interrogator passes through the gratings, a specific wavelength is reflected. A change in the reflected wavelength is proportional to the applied strain and a simultaneous temperature change. The mechanical strain $\varepsilon_{\rm mech}$ can be computed using eqn. (1) (Magne et al., 1997).

$$arepsilon_{
m mech} = rac{1}{k} igg(\ln rac{\lambda_1}{\lambda_0} - S_1 \Delta T igg) - (lpha_c - lpha_f) \Delta T$$

where $\lambda_{\rm l}$ is the current FBG wavelength, $\lambda_{\rm 0}$ is the wavelength at the outset of measurement, k is the gauge sensitivity factor, $S_{\rm l}$ is the temperature sensitivity factor, $\alpha_{\rm o}$ is the coefficient of thermal expansion (CTE) of concrete (taken as 12 $\mu \epsilon/^{\circ}$ C; Revilla-Cuesta et al., 2022) and $\alpha_{\rm p}$ is the CTE of the fibre (0.5 $\mu \epsilon/^{\circ}$ C as provided by the manufacturer).

Changes in temperature were computed from the thermal FBG wavelengths by making ΔT the subject of eqn. (1), setting $\epsilon_{\rm mech}$ -0 and replacing the CTE of concrete with that of aluminium (20.92 $\mu\epsilon$ /°C; Hensman & Sheil, 2023).

WWSGs use a magnetic field to induce oscillations in a tensioned steel wire. A change in length of the wire produces a corresponding change in frequency. Additionally, differences between the CTEs of concrete and the strain gauge gives rise to a spurious strain (Neild et al., 2005), which can be corrected for using eqn (2).

$$\varepsilon_t = G(f_1^2 - f_0^2) + (\alpha_g - \alpha_c)(\Delta T) \tag{2}$$

where $\epsilon_{\rm t}$ is the total strain, G is the gauge calibration factor, $\alpha_{\rm c}$ is the CTE of the gauge (quoted as 12.2 $\mu{\rm e}/{\rm ^{\circ}C}$ by the manufacturer), $f_{\rm l}$ and $f_{\rm o}$ are the current and zero-stress frequency measurements respectively. Mechanical strains can then be computed using eqn (3).

$$\varepsilon_{mech} = \varepsilon_t - \alpha_c \Delta T$$
(3)

EXAMPLE RESULTS FROM IP1

Temperatures during construction

Changes in temperature inferred from the WSG thermistors and thermal FBGs during construction are plotted in Fig 5. The thermal FBG temperatures at the NE location plot slightly below those from the E thermistors. This can be attributed to the insulating effect of the bubble wrap around the thermal FBGs (Hensman & Sheil, 2023). Furthermore, the south thermistors were not exposed to direct sunlight when the sensors were zeroed (i.e. when the pipe was above ground),

so the E thermistors were considered more representative of the overall pipe temperature. For these reasons, the average temperature data from the thermistors at the E cardinal point was favoured for calculating strains.

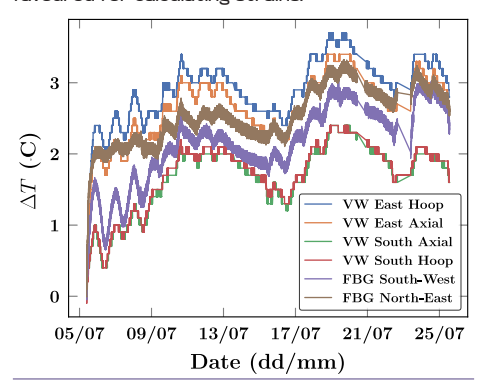


Figure 5 Changes in temperatures during the pipeline construction process

Axial strains during construction

The FBG and VWSG axial strains at the S and E positions are plotted against jacked distance in Figs. 6a and 6b respectively. In this figure, compressive strains are represented as negative. The point at which IPI enters the horizontal curve (i.e. 90.7 + 99 \approx 190m) is also identified.

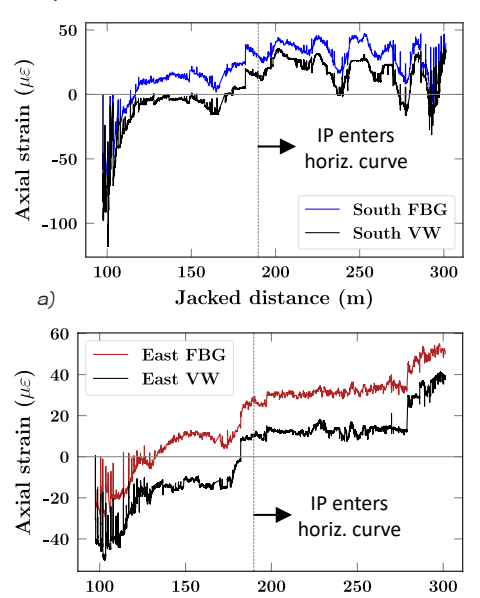


Figure 6 FBG (uncorrected) and VWSG axial strains during construction at (a) South and (b) East cardinal points

Jacked distance (m)

While both sensor types were zeroed above ground prior to incorporation of IPI within the pipe train, it is apparent that the strain traces become offset from each other at a very early stage of jacking, although they follow a very similar trend for the remainder of the drive. An average offset between FBG and VWSG strains was calculated (for S and E sensors) and all FBG strain magnitudes were adjusted by this amount.

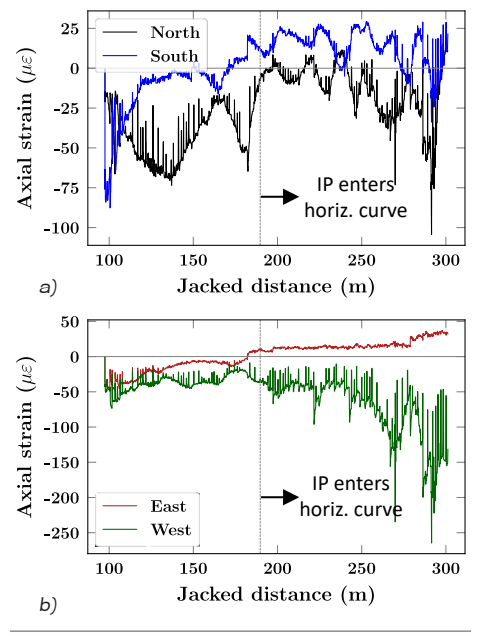


Figure 7 FBG (corrected) axial strains during construction at (a) North-South (b) East-West cardinal points

The variation in (corrected) FBG axial strains around the pipe circumference is plotted against jacked distance in Fig. 7. Data from opposite cardinal points are plotted on the same graph; Fig. 7a displays the data from the N and S cardinal points, whereas Fig. 7b shows the data from the E and W cardinal points.

In Fig. 7a, during the initial few metres after IP1 was introduced into the tunnel, the S axial (SA) sensor registered higher compressive strains than the N axial (NA) sensor. This is consistent with the bottom of the pipe being initially restrained due to contact with surrounding soil, i.e. the pipe slid along the bottom of the excavated borehole. However, as IP1 advanced further into the tunnel, a steady decrease in SA and increase in NA compressive strains respectively was observed, indicating that the pipe became buoyant. From \$170 m, tensile strains were recorded at the SA position for most of the remainder of the drive.

It is evident from Figs. 7a and 7b that opposite cardinal points (N-S and E-W) exhibit contrasting behaviour throughout the drive. When a sensor experienced relative compression, the opposite one underwent relative tension, and vice versa. Therefore, the pipe was subjected to bending along both axes. Once the pipe entered the horizontal curve, the E and W strains diverge (Fig. 7b), indicating that the pipe undergoes further bending.

The requirement for the offset in FBG strain magnitudes discussed may be eliminated by performing a field calibration of FBG sensors, using the VWSG data. This will be considered in a future publication.

CONCLUSION

This paper details the deployment of an instrumented pipe incorporating FBG and VWSG sensors in a curved PJ drive through alluvium and glacial till. The following conclusions can be drawn:

- Axial strains recorded using FBG and VWSG show similar patterns when plotted against jacked distance. Differences in magnitude may be addressed through field calibration of the former.
- The axial strain data implies that IP1 was buoyant for most of the drive.
- Bending arose in both the N-S and E-W directions, which caused tensile stresses in the pipe. These need to be considered in RC pipe design.
- At least four sensors should be used around the pipe circumference to capture the complete temperature distribution.
- If FBGs are to be used as thermal sensors, the blocks should be made of the same material as the structure, in which case wrapping the thermal FBGs in foam (which was problematic here) would not be required.

ACKNOWLEDGEMENTS

The first author is funded by Research Ireland. All authors acknowledge the support of Tracey Concrete Ltd and Ward and Burke Construction Ltd. for casting and deployment of the instrumented pipe.

REFERENCES

FBGS. (2019). Instruction Manual. www.fbgs.com

- Hensman, P. J., & Sheil, B. B. (2023). Monitoring Strains and Temperatures in a Deep Excavation Base Slab Using Fibre-Optic Bragg Gratings. Int. Conf. on Geotechnics for Sustainable Infrastructure Development. 1967-1981.
- Magne, S., Rougeault, S., Vilela, M., & Ferdinand, P. (1997). State-of-strain evaluation with fiber Bragg grating rosettes: application to discrimination between strain and temperature effects in fiber sensors. Applied Optics, 36(36), 9437-9447.
- Neild, S. A., Williams, M. S., & McFadden, P. D. (2005). Development of a vibrating wire strain gauge for measuring small strains in concrete beams. Strain, 41(1), 3-9.
- Revilla-Cuesta, V., Skaf, M., Santamaría, A., Espinosa, A. B., & Ortega-López, V. (2022). Self-compacting concrete with recycled concrete aggregate subjected to alternating-sign temperature variations: Thermal strain and damage. Case Studies in Construction Materials, 17.
- Wadood, A., McCabe, B. A., & Sheil, B. B. (2025). Field monitoring and instrumentation in microtunnelling /pipe jacking: A review and future directions. Underground Space, 22, 225-240.